Journal of Applied Physics

Dynamic magnetization of ε-Fe_2O_3 in pulse field: Evidence of surface effect

Cite as: J. Appl. Phys. **117**, 063908 (2015); https://doi.org/10.1063/1.4907586
Submitted: 21 October 2014 . Accepted: 25 January 2015 . Published Online: 12 February 2015

D. A. Balaev, I. S. Poperechny, A. A. Krasikov, K. A. Shaikhutdinov, A. A. Dubrovskiy, S. I. Popkov, A. D. Balaev, S. S. Yakushkin, G. A. Bukhtiyarova, O. N. Martyanov, and Yu. L. Raikher

Dynamic magnetization of ε-Fe_2O_3 in pulse field: Evidence of surface effect

D. A. Balaev,[1,2,a)] I. S. Poperechny,[3,4] A. A. Krasikov,[2] K. A. Shaikhutdinov,[1] A. A. Dubrovskiy,[1] S. I. Popkov,[1] A. D. Balaev,[1] S. S. Yakushkin,[5] G. A. Bukhtiyarova,[5] O. N. Martyanov,[5] and Yu. L. Raikher[3,6]

[1]*Kirensky Institute of Physics, Russian Academy of Sciences, Siberian Branch, Krasnoyarsk 660036, Russia*
[2]*Siberian Federal University, Krasnoyarsk 660041, Russia*
[3]*Institute of Continuous Media Mechanics, Russian Academy of Sciences, Ural Branch, Perm 614013, Russia*
[4]*Perm National Research Polytechnic University, Perm 614990, Russia*
[5]*Boreskov Institute of Catalysis, Russian Academy of Sciences, Siberian Branch, Novosibirsk 630090, Russia*
[6]*Ural Federal University, Ekaterinburg 620083, Russia*

(Received 21 October 2014; accepted 25 January 2015; published online 12 February 2015)

The magnetization dynamics of ε-Fe_2O_3 nanoparticles with an average size of about 9 nm is investigated. From comparison of the hysteresis loops obtained in quasi-static conditions and under pulse fields with amplitudes up to 200 kOe and pulse lengths 8–32 ms, it follows that the effective coercivity increases considerably with the variation rate of the imposed magnetic field. A theoretical explanation of this behavior is proposed. The model takes into account the superparamagnetic effects as well as the fact that magnetic anisotropy of the nanoparticles, along with the bulk term, includes a surface contribution. The latter, being of minor importance for the observed magnetic behavior of 25–100 nm particles, becomes essential when the particle size is below 10 nm. From the experimental data, a reference value of the surface anisotropy of nanodisperse ε-Fe_2O_3 is established, and evidence is presented to the effect that below 300 K this contribution does not significantly depend on temperature. © *2015 AIP Publishing LLC*. [http://dx.doi.org/10.1063/1.4907586]

I. INTRODUCTION

The polymorphic modification of iron oxide ε-Fe_2O_3 was first reliably identified in 1998.[1] In modern view, it is a canted ferrimagnet with the magnetic ordering temperature of 500–585 K.[2–11] This phase is usually synthesized in the nanodisperse form, see, for example, Refs. 8 and 9. Among all other iron oxides, a unique specific feature of ε-Fe_2O_3 is the high level of coercivity H_c being about 20 kOe at room temperature for grains 25–100 nm in size.[2,3,5,12,13] However, the H_c value of such particles sharply decreases below 150 K. This fact, along with the anomalies in the temperature dependence of magnetization between 80 and 150 K,[12,14] is considered as related to a certain magnetic transition, the nature of which is still argued.[3,6,9,10]

The strong coercivity of ε-Fe_2O_3 predetermines the application prospects of these nanoparticles. First, it is magnetic recording and data storage.[10,15] The relatively low remanent magnetization (∼10 emu/g (Ref. 10)) is not a serious limiting factor nowadays given the high sensitivity of the giant magnetoresistance-based reading devices. Second, these are permanent magnets with super-high coercivity, e.g., the ε-Fe_2O_3 nanoparticles embedded in silica matrices. Although the low level of remanent magnetization is a considerable drawback if to use these oxides as such, their combination with magnetically soft particles or matrices seems promising for making composites of the exchange spring type.

The most fascinating application area for the nanodisperse ε-Fe_2O_3 is radio-optics. As the particles possess very high H_c, their Larmor frequency in the absence of an external field, i.e., the frequency of intrinsic (natural) ferromagnetic resonance, is about 200 GHz. This is millimeter wavelength range, for which the magnetoactive media are in deficiency and, thus, in great demand.[7] Pure ε-Fe_2O_3 nanodispersions as well as those doped with indium[6,11] and ruthenium,[15] being capable of high absorption rates and strong Faraday effect, might fit very well the sub-THz communication technology requirements for the materials for attenuators and phase rotators.[15]

Since all the prospective applications of nanodisperse ε-Fe_2O_3 are concerned exclusively with its unique magnetic hardness, the practical knowledge of magnetic anisotropy of the material is of paramount interest. In order to advance along this line, hereby we: (i) investigate the dynamics of magnetization and re-magnetization of nanoparticles and (ii) distinguish and estimate the bulk and surface contributions to the particle effective anisotropy. This is done by measuring the dynamic magnetic hysteresis (DMH) loops of ε-Fe_2O_3 nanoparticles in a quasi-harmonic field. We show that taking into account the superparamagnetic effect ever present in polydisperse nanoparticle assemblies, one is able to consistently interpret the results, and make some conclusions on the temperature dependence of the anisotropy constants.

II. EXPERIMENTAL DETAILS

A. Samples

Samples of ε-Fe_2O_3 in a porous silica gel matrix were synthesized by incipient wetness impregnation with the Fe(II) sulphate solutions[16,17] and subsequent drying at 110 °C and calcination at 900 °C for 4 h. According to the X-

a)Electronic mail: dabalaev@iph.krasn.ru

ray data,[16] this technique yields the ε-Fe_2O_3 particles free of any other iron oxide polymorphic phases. For this study ε-Fe_2O_3/SiO_2 samples were prepared with iron ion content about 7.4 wt. %, hereinafter we refer to them as 7FS. The magnetic properties of the samples with a lower Fe content and, correspondingly, smaller size have been studied before in Refs. 17 and 18.

High resolution transmission electron microscopy (HRTEM) investigations of the 7FS samples were performed using a JEOL JEM-2010 microscope with resolution up to 1.4 Å. The size distribution was estimated by a statistical count of particles from several frames taken from different parts of the sample. The results are shown in Fig. 1 together with their approximation done with the aid of a log-normal function, whose parameters are $d_0 = 7.3$ nm and $s = 0.7$. The calculated average size is 8.6 nm, the width of the 95% interval is ±6.15 nm.

B. Magnetic measurements

1. Quasistatic magnetic properties

Quasistatic magnetization loops $M(H)$ were recorded on a PPMS-6000 measurement system (Quantum Design) in the fields ±90 kOe at temperatures of 77.4 K and 300 K. The temperature dependence of $M(T)$ was determined by means of zero-field cooling (ZFC) and FC tests. In the range of 4.2–300 K, a vibrating sample magnetometer was used.[19] In the range of 300–600 K, the data were obtained using a high-temperature appliance of the PPMS-6000 facility. In those measurements, a powder sample glued to a sapphire substrate was kept under high vacuum: 10^{-10} Torr.

2. Magnetization in pulse fields

The complete DMH loops of nanodispersed ε-Fe_2O_3 cannot be measured by standard techniques, since in this system the $M(H)$ curve exhibits distinct signs of saturation only in fields ranging 50–60 kOe (Refs. 2, 3, 5, 12, and 13). Since the harmonic magnetic field of such an amplitude is technically unattainable, we use a pulse field induced by battery discharge through a solenoid. This is done on an original setup at the Laboratory of High Magnetic Fields, Kirensky Institute of Physics, Russian Academy of Sciences, Siberian Branch. The field is induced by discharging a capacitor battery through a copper solenoid. Technically, it is an LC contour, in which the self-oscillating process is initiated by a thyristor opening after charging the capacitors to a given voltage. Usually, the oscillations in such setups are stopped by a thyristor right after the first half-wave. Meanwhile, to get a complete magnetization loop, one needs at least one full wave. To provide the second half-wave, diodes are connected inverse-parallel to the thyristor. In such a way, one gets a field pulse of a sufficient amplitude and with the shape close to that of a single period of harmonic oscillation.

The magnetic response is taken by a pickup system of a set of compensated coaxial coils surrounding the sample. The output signal of the coils is amplified and recorded by a digital storage oscilloscope. The sample magnetization is determined by processing the difference between signals taken from the induction sensor with and without the sample under the same electric current pulses.

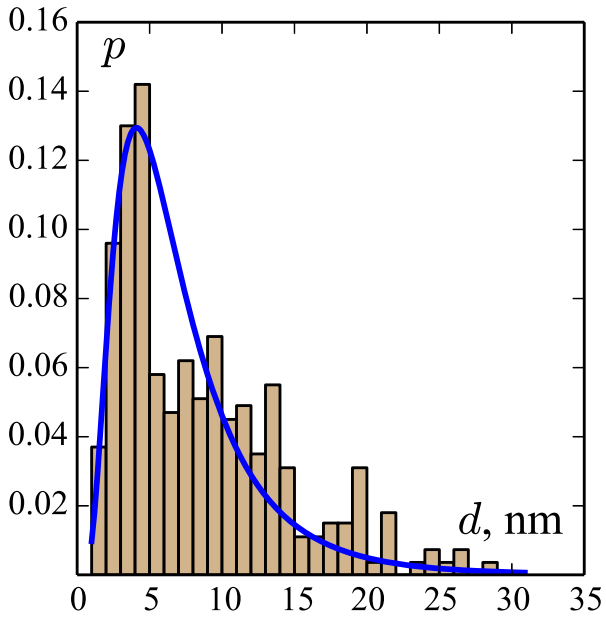

FIG. 1. HRTEM histogram for the 7FS sample and the lognormal function with the parameters $d_0 = 7.3$ nm and $s = 0.7$.

III. EXPERIMENTAL RESULTS

Figure 2 shows the temperature dependence of magnetization measured in different fields under FC/ZFC conditions at temperatures up to 600 K. The obtained dependencies $M(T)$ are irreversible: the ZFC and FC data do not coincide, at least below 300 K. It can be seen that the transition to the magnetically ordered state occurs at 500 K in agreement with the data reported in Refs. 2–11.

In the temperature range of 100–150 K, the $M(T)$ curves in both ZFC and FC regimes display a maximum. Its position does not depend on the field strength in the 1–10 kOe range, displaying a slight shift in the 100 Oe–1 kOe interval, see inset in Fig. 2. This evidences that the $M(T)$ maximum is not

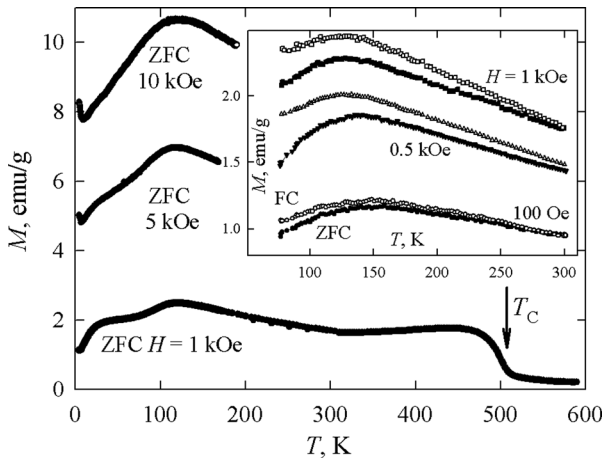

FIG. 2. Temperature dependencies of magnetization for the 7FS sample under different external fields; arrow indicates the transition point to the magnetically ordered state; inset shows the data obtained via ZFC (closed symbols) and FC (open symbols) protocols.

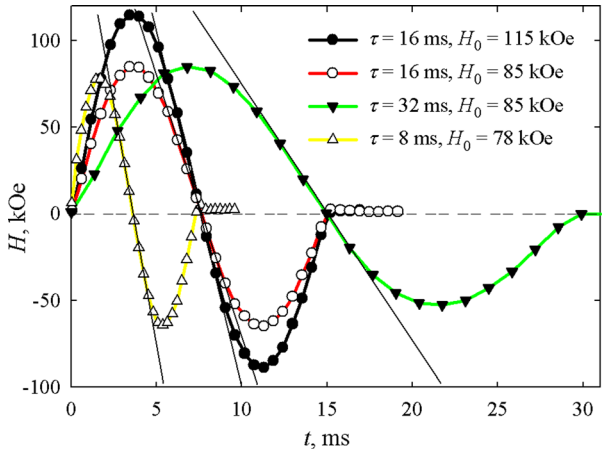

FIG. 3. Time-change of the field inside the solenoid for different τ's; thin straight lines (tangents) illustrate determination of the field variation rate $(dH/dt)_{max}$ at the instant of the sample remagnetization, i.e., when the magnetization changes its sign.

caused by superparamagnetic blocking and is due to the magnetic transition in ε-Fe_2O_3.[12]

Measurements of the DMH loops on 7FS sample in pulse fields were performed at temperatures of 77.4 K and 300 K. The pulse lengths were specified by changing capacitance of the battery and amounted to $\tau = 8$, 16, and 32 ms. The magnetic field amplitude H_0 was controlled by the initial charge of the battery and ranged from 80 to 200 kOe. The field grew from zero to H_0, then went down to a negative value somewhat smaller than the $|H_0|$ (Fig. 3), and finally decreased to zero.

Typical DMH loops are shown in Fig. 4 together with the quasistatic (DC) data obtained using a vibrating sample magnetometer with the field variation rate about 20 Oe/s. In the dynamic regime, we define the effective coercivity H_c as the value of the field at the point, where the curve $M(H_c)$ intersects the abscissa axis in the negative region. As can be seen from Fig. 4, thus defined values of H_c obtained with pulse remagnetization exceed by far the quasistatic coercivity. Moreover, Fig. 4(a) where the DMH loops measured at different τ but similar H_0 are presented, evidences the increase of H_c with diminution of the pulse duration. If, on the contrary, the pulse duration is kept constant, then H_c increases with the field amplitude, see Fig. 4(b).

To describe the dependence of H_c on the pulse length τ and amplitude H_0, it is convenient to use the parameter $(dH/dt)_{max}$ that is the maximal variation rate of the applied field. For the harmonic field that we use to simulate the pulse process, one has $(dH/dt)_{max} = \omega H_0 = 2\pi H_0/T$, i.e., the ratio of the field amplitude to the pulse duration. Under experimental conditions, the value of this parameter is determined as the slope of a tangent of $H(t)$ function at the point where it intersects the abscissa axis, see Fig. 3.

Dependencies of the effective coercivity H_c on $(dH/dt)_{max}$ at $T = 300$ K and $T = 77.4$ K are shown in Figs. 5(a) and 5(b), respectively; there the points visually positioned on the ordinate axis render the results of the quasistatic measurement (vibrating sample magnetometry). The data shown in Fig. 5 were obtained under the field amplitudes $H_0 \geq 70$ kOe and, thus, characterize the major dynamic hysteresis loops.

IV. THEORETICAL MODEL

The above-mentioned preparation technique suggests that ε-Fe_2O_3 nanoparticles are rather uniformly distributed in the bulk of a sample. Since the mass fraction of iron is relatively small (7.4 wt. %), in the calculation of the magnetization curves one may neglect the interparticle coupling and take into account only the interaction of the particles with the applied field. A consistent theory of the dynamic remagnetization of noninteracting anisotropic single-domain particles with allowance for thermal fluctuations is built in Ref. 20. Here, we use its simplified variant termed *semi-adiabatic* (SA) approximation developed in Ref. 21. Estimating applicability of the SA model to the nanoparticles of the size about 10 nm, see Fig. 1, one finds that it works at the frequencies up to 1 MHz. In our experiment the shortest pulse duration is 8 ms, so that the equivalent cyclic frequency f does not exceed 125 Hz; apparently, the SA requirement is well satisfied.

To interpret the measurement results, we model the ε-Fe_2O_3 dispersion by an assembly of independent spherical

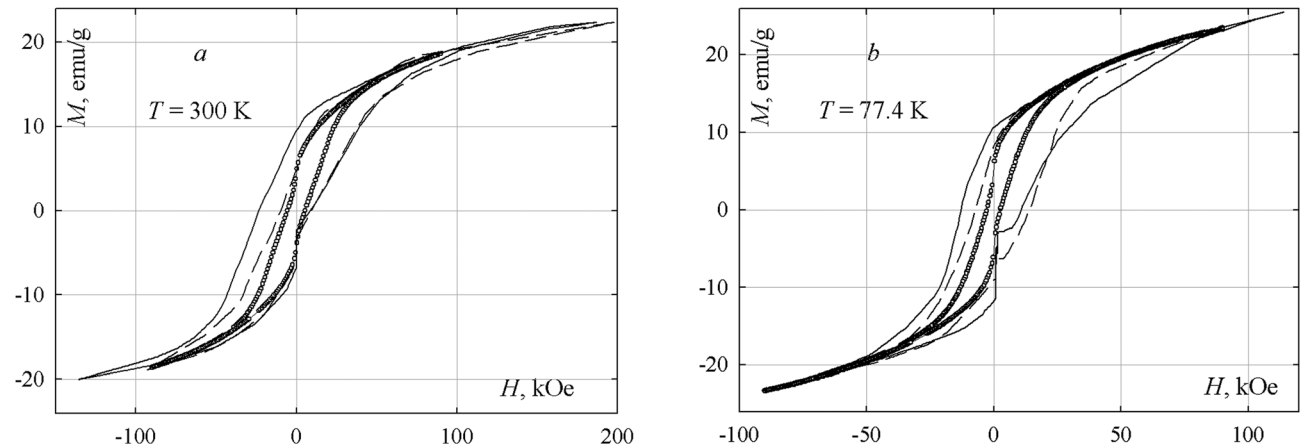

FIG. 4. Typical dependencies $M(H)$ obtained in quasistatic (symbols) and pulse (lines) fields at 300 (a) and 77.4 K (b). The field pulse parameters are $\tau = 16$ ms, $H_0 = 186$ kOe (solid line) and $\tau = 32$ ms, $H_0 = 200$ kOe (dashed line) for (a); $\tau = 16$ ms, $H_0 = 115$ kOe (solid line) and $\tau = 16$ ms, $H_0 = 84$ kOe (dashed line) for (b).

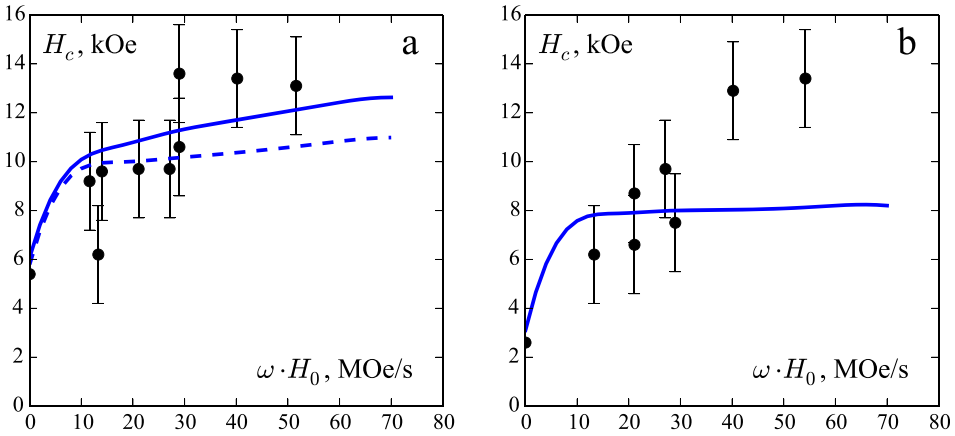

FIG. 5. Dynamic coercivity vs variation rate of the magnetic field; dots with errorbars mark experimental data; solid lines are calculated via SA model using lognormal distribution with the parameters given in Fig. 1; (a): $T = 300\,\mathrm{K}$, $K_V = 4.5 \times 10^6\,\mathrm{erg/cm^3}$, and $K_S = 0.1\,\mathrm{erg/cm^2}$ and (b): $T = 77.4\,\mathrm{K}$, $K_V = 5 \times 10^2\,\mathrm{erg/cm^3}$, and $K_S = 0.27\,\mathrm{erg/cm^2}$. Dashed line shows fitting with the SA model at $K_V = 5.1 \times 10^6\,\mathrm{erg/cm^3}$, $K_S = 0$, i.e., without surface anisotropy.

particles with uniaxial magnetic anisotropy which comprises two contributions: bulk and surface. The particle magnetic energy related to the first one is

$$E_V = -K_V V(\boldsymbol{e} \cdot \boldsymbol{n})^2, \tag{1}$$

where K_V is the bulk anisotropy constant, V the particle volume, and $\boldsymbol{e}$ and $\boldsymbol{n}$ are unit vectors of the magnetic moment and easy magnetization axis, respectively. The necessity to account for the surface energy is due to the following. As seen from the HRTEM histogram in Fig. 1, for the majority of particles in the system under study, their diameter d does not exceed 5 nm. Containing a large fraction of spins with incomplete coordination, the ferrite grains of this size possess a significant surface magnetic anisotropy, see Refs. 22 and 23. Besides that, particularly for nano-ε-Fe_2O_3, a clear qualitative evidence of surface spin pinning is reported in Ref. 12.

A simple model for this type of anisotropy is built on Néel's original considerations, see Refs. 24–26, for example. In the notations here used, the corresponding term in the particle energy is

$$E_S = -K_S S(\boldsymbol{e} \cdot \boldsymbol{n})^2, \tag{2}$$

where S is the particle lateral area and K_S the surface anisotropy constant. As seen from (1) and (2), the directions of the easy axes in the bulk and on the surface are assumed to coincide, so that the particle anisotropy energy may be arranged to the form

$$E_A = E_K + E_S = -K_{\mathrm{eff}} V(\boldsymbol{e} \cdot \boldsymbol{n})^2, \tag{3}$$

where, as in Ref. 27, the effective constant

$$K_{\mathrm{eff}} = K_V + 6K_S/d, \tag{4}$$

is introduced. Then the entire orientation-dependent part of the particle energy in external magnetic field $\boldsymbol{H}$ is

$$U = -\boldsymbol{\mu} \cdot \boldsymbol{H} - K_{\mathrm{eff}}(\boldsymbol{e} \cdot \boldsymbol{n})^2, \tag{5}$$

with $\boldsymbol{\mu}$ being the particle magnetic moment. Since preparation of the ε-Fe_2O_3 dispersion suggests no preferential orientations of the particle axes, we take that in the model statistical ensemble they are distributed at random.

In an applied AC field, the energy of a particle and, consequently, the orientation of its magnetic moment are functions of time. According to the theory,[21] the averaged projection of the magnetic moment onto the direction $\boldsymbol{h}$ of linearly polarized field is presented as a sum

$$\mu(t) = \mu_0[H(t)] + \mu_1(t). \tag{6}$$

The first term, $\mu_0[H(t)]$, is the "adiabatic" component, i.e., the equilibrium value that $\boldsymbol{\mu}$ would have had in the field with instantaneous strength $H(t)$. The second term, μ_1(t), is the retarded part. As shown in Ref. 21, it is determined by the relation

$$\mu_1(t) = A_1(t) \cdot \int (\boldsymbol{\mu} \cdot \boldsymbol{h})\, F_1(\boldsymbol{e}, t) d\Omega, \tag{7}$$

where integration spans over all orientations of the magnetic moment. Function $F_1(\boldsymbol{e}, t)$ in the integrand has a quasi-Boltzmann form

$$F_1(\boldsymbol{e}, t) = \begin{cases} [Z_1(t)]^{-1} \exp[-U(\boldsymbol{e}, t)/k_B T], & \boldsymbol{e} \in \Omega_1; \\ -[Z_2(t)]^{-1} \exp[-U(\boldsymbol{e}, t)/k_B T], & \boldsymbol{e} \in \Omega_2. \end{cases} \tag{8}$$

Partition integrals $Z_1(t)$ and $Z_2(t)$ are evaluated in the regions $\Omega_1 = \{0 \le \vartheta < \vartheta_s,\ 0 \le \varphi \le 2\pi\}$ and $\Omega_2 = \{\vartheta_s \le \vartheta < \pi,\ 0 \le \varphi \le 2\pi\}$, respectively; here ϑ_s is the polar coordinate of the saddle point of potential (5).

Coefficient $A_1(t)$ in (7) is the solution of the first-order differential equation

$$\frac{dA_1}{dt} + \frac{\lambda_1(t)}{2\tau_D} A_1 = -\frac{d}{dt}\left(\frac{Z_1 - Z_2}{Z_1 + Z_2}\right), \tag{9}$$

where $\lambda_1(t)$ is the smallest eigenvalue of the Brown equation[28] evaluated for the field strength $H(t)$, and $\tau_D = (K_{\mathrm{eff}} V/k_B T)\,\tau_0$ is the reference time of thermal diffusion of the particle magnetic moment, see Ref. 29, for example; the attempt time τ_0 is set to $10^{-9} s$.

V. COMPARISON WITH THE EXPERIMENT

When modeling the experiment described in Sec. III, we assume that the applied field follows the harmonic law $H(t) = H_0 \cos \omega t$ correlating the frequency to the pulse

length τ as $\omega = 2\pi/\tau$. The dependence $\mu(t)$ for a given direction $\boldsymbol{n}$ of the particle anisotropy axis is obtained by numerical integration of Eqs. (6)–(9). This solution, upon eliminating the time from the pair of relations $M(t) = \mu(t)/V$ and $H(t)$, yields the magnetization curve $M(H, \boldsymbol{n})$. Then, by repeating that procedure, the averaging of function $M(H)$ is performed with respect to two parameters: (i) the orientation of anisotropy axes, which is assumed to be random and (ii) the particle size, using the lognormal distribution of Fig. 1. This yields the magnetization loop $M(H)$ for a polydisperse ensemble of non-aligned ε-Fe_2O_3 nanoparticles. From it, the dynamic coercivity H_c is determined via the condition $M(H_c) = 0$. Evidently, since H_c possesses a relaxational contribution, it depends on the field "period" τ.

Comparison of the measurement results against the SA theoretical dependencies $H_c(\omega H_0)$ is presented in Fig. 5. When fitting, we take into account the dramatic difference in the values of bulk anisotropy constant in ε-Fe_2O_3 at room and low temperatures. For 300 K, we set $K_V = 4.5 \times 10^6$ erg/cm^3 taking it from the reference range $K_V \sim 5 \times 10^6$ erg/cm^3 established in a number of works[10,12,14,15] where the particles of the size about 25–100 nm were studied. According to the same data, around 85 K the value of K_V falls down by about four orders of magnitude. This temperature is close to that of our measurement: 77.4 K. Assuming the same extent of reduction of the bulk anisotropy in our particles, we set $K_V = 5 \times 10^2$ erg/cm^3.

The quantitative contribution of the surface anisotropy in magnetodynamics of nano-ε-Fe_2O_3, as far as we know, is introduced for the first time. As mentioned, the importance of the surface term follows with necessity from the smallness of the particle average size (9 nm). In larger nanograins, like those of Refs. 12 and 15, the surface effect is much lower and, thus, is hard to measure. As the nanoparticles under study have homogeneous chemical content (no core-shell structure), the surface anisotropy is mostly associated with the incomplete environment and, thus, non-uniform arrangement of spins on the outer border of the particles. Such a K_S is of the exchange origin, and one may expect that below the Curie point this parameter should at the most grow gradually with the temperature decrease. That is why for the surface energy density at room temperature we set $K_S = 0.1$ erg/cm^2 taking it from the typical range inherent to iron oxides.[23,26,30] Certainly, it is a naive guess given the complex magnetic structure of nano-ε-Fe_2O_3. However, even this simple assumption proves to be an essential step in right direction. In Fig. 5(a) that renders the data at 300 K, the solid line gives the result of fitting with $K_S = 0.1$, while the dashed one corresponds to the attempt with $K_S = 0$. As seen, the curve with a finite K_S yields a substantially better agreement.

The interpretation of the low-temperature case shown in Fig. 5(b) is yet more instructive. Note that the ratio of quasi-static values $H_c(300\,K)/H_c(77\,K)$ in our experiment (particle size 9 nm) turns out to be only about 2.5 instead of the above-mentioned 30 in Ref. 12, where the particle size is 25–100 nm. It is clear that the bulk anisotropy, as itself, which in this temperature interval ranges $K_V \sim 10^3$ erg/cm^3, fails completely to account for the evidence. The situation changes as soon as the surface term moderately increasing with the particle cooling is included in Eq. (4). As Fig. 5(b) shows, setting K_S to a quite reasonable value 0.27 erg/cm^2 suffices to fit fairly well the frequency dependence of H_C at low-temperature for the $(dH/dt)_{max}$ values up to 40 MOe/s.

VI. DISCUSSION

Remagnetization of ε-Fe_2O_3 nanoparticles is investigated by a pulse method that enables one to achieve quite high magnetic fields. The magnetic hysteresis loops are obtained and the effective coercivity is measured under the field variation rates from 20 Oe/s (quasistatic mode) to 60 MOe/s. The theoretical interpretation is based on the SA approximation that accounts for the long-lived superparamagnetic relaxation mode.

The SA model is compared with the experimental evidence at two temperatures, at which the nanoparticles of ε-Fe_2O_3 have rather different anisotropic properties. Analysis of the 300 K and 77.4 K measurements of H_C on a unified basis reveals the essential role that the surface anisotropy plays in formation of coercivity of nanodisperse ε-Fe_2O_3 with the particle size $\sim$10 nm.

As the surface term scales proportionally to $1/d$, it is the more relevant the smaller the particles. A simple estimate is instructive. Let for simplicity be $K_V = 0$. Setting the particle diameter to 5 nm, and, as found, $K_S \sim 0.1$ erg/cm^2, from expression (4) for the effective anisotropy constant one gets $K_{eff} = 6K_S/d \approx 10^6$ erg/cm^3. Taking $M_s \approx 20$ emu/g for the specific saturation magnetization[10] and $\rho \approx 5$ g/cm^3 for the specific gravity, we obtain the equivalent coercivity as large as $H_c = 2K_{eff}/(\rho M_s) \sim 20$ kOe. This means that even in the entire absence of bulk anisotropy, the surface term alone is able to ensure the high coercivity of the particles.

The surface magnetic anisotropy is of utter importance for the most interesting application of nanodisperse ε-Fe_2O_3, viz., millimeter wavelength radio-optics. Indeed, as the afore-given estimate shows, for the 5 nm particles the frequency of intrinsic ferromagnetic resonance (IFMR) even at $K_V = 0$ still lies in the sub-THz band. Moreover, upon combining the bulk and surface anisotropies of such particles, one can enhance the IFMR frequency of a randomly oriented nanodispersion about 50% over the highest result (31 kOe) attainted only after orientational texturizing of 20–40 nm particles, as is reported in Ref. 15. Note also that if, as our model assumes, the surface term grows with the temperature diminution, then high coercivity of ε-Fe_2O_3 nanodispersion could be retained even in the temperature range around 80 K, where the bulk anisotropy almost disappears. The above-mentioned just moderate reduction of quasi-static H_C that we encountered when cooling the sample from 300 to 77 K, strongly supports this inference.

VII. CONCLUSIONS

With the aid of the semi-adiabatic model the essential role of surface anisotropy in the observed magnetic properties of finely nanodisperse ε-Fe_2O_3 is unambiguously revealed. However, at present the agreement with the data is rather semi-quantitative than precise. In particular, we note the deviation between theoretical and measurement results at

77.4 K for $\omega H_0 > 40$ MOe/s. In our view, this discrepancy points out the shortage of fundamental knowledge on the magnetic structure of nano-ε-Fe_2O_3 and makes the studies of that a challenging issue.

ACKNOWLEDGMENTS

The work was supported by RFBR Grant Nos. 14-02-96002 and 12-02-00897, and project MIG S26/617 from the Ministry of Education and Science of Perm Region.

[1]E. Tronc, C. Chaneac, and J. P. Jolivet, "Structural and magnetic characterization of ε-Fe_2O_3," J. Solid State Chem. **139**, 93–104 (1998).
[2]M. Popovici, M. Gich, D. Niznansky, A. Roig, C. Savii, L. Casas, E. Molins, K. Zaveta, C. Enache, J. Sort, S. de Brion, G. Chouteau, and J. Nogués, "Optimized synthesis of the elusive ε-Fe_2O_3 phase via sol-gel chemistry," Chem. Mater. **16**, 5542–5548 (2004).
[3]M. Kurmoo, J.-L. Rehspringer, A. Hutlova, C. D'Orlans, S. Vilminot, C. Estournes, and D. Niznansky, "Formation of nanoparticles of ε-Fe_2O_3 from yttrium iron garnet in a silica matrix: An unusually hard magnet with a Morin-like transition below 150 K," Chem. Mater. **17**, 1106–1114 (2005).
[4]E. Tronc, C. Chaneac, J. P. Jolivet, and J. M. Greneche, "Spin collinearity and thermal disorder in ε-Fe_2O_3," J. Appl. Phys. **98**, 053901 (2005).
[5]S. Sakurai, J. Jin, K. Hashimoto, and S. Ohkoshi, "Reorientation phenomenon in a magnetic phase of ε-Fe_2O_3 nanocrystal," J. Phys. Soc. Japan **74**, 1946–1949 (2005).
[6]S. Sakurai, S. Kuroki, H. Tokoro, K. Hashimoto, and S. Ohkoshi, "Synthesis, crystal structure, and magnetic properties of ε-$In_xFe_{2-x}O_3$ nanorod-shaped magnets," Adv. Funct. Mater. **17**, 2278–2282 (2007).
[7]A. Namai, S. Sakurai, M. Nakajima, T. Suemoto, K. Matsumoto, M. Goto, S. Sasaki, and S. Ohkoshi, "Synthesis of an electromagnetic wave absorber for high-speed wireless communication," J. Am. Chem. Soc. **131**, 1170–1173 (2009).
[8]S. Sakurai, A. Namai, K. Hashimoto, and S. Ohkoshi, "First observation of phase transformation of all four Fe_2O_3 phases ($\gamma \rightarrow \varepsilon \rightarrow \beta \rightarrow \alpha$-phase)," J. Am. Chem. Soc. **131**, 18299–18303 (2009).
[9]L. Machala, J. Tucek, and R. Zboril, "Polymorphous transformations of nanometric iron(III) oxide: A review," Chem. Mater. **23**, 3255–3272 (2011).
[10]J. Tucek, R. Zboril, A. Namai, and S. Ohkoshi, "ε-Fe_2O_3: An advanced nanomaterial exhibiting giant coercive field, millimeter-wave ferromagnetic resonance, and magnetoelectric coupling," Chem. Mater. **22**, 6483–6505 (2010).
[11]K. Yamada, H. Tokoro, M. Yoshikiyo, T. Yorinaga, A. Namai, and S. Ohkoshi, "The phase transition of ε-$In_xFe_{2-x}O_3$ nanomagnets with a large thermal hysteresis loop," J. Appl. Phys. **111**, 07B506 (2012).
[12]M. Gich, A. Roig, C. Frontera, E. Molins, J. Sort, M. Popovici, G. Chouteau, D. M. y Marero, and J. Nogués, "Large coercivity and low-temperature magnetic reorientation in ε-Fe_2O_3 nanoparticles," J. Appl. Phys. **98**, 044307 (2005).
[13]S. Ohkoshi, S. Sakurai, J. Jin, and K. Hashimoto, "The addition effects of alkaline earth ions in the chemical synthesis of ε-Fe_2O_3 nanocrystals that exhibit a huge coercive field," J. Appl. Phys. **97**, 10K312 (2005).
[14]Y. C. Tseng, N. M. Souza-Neto, D. Haskel, M. Gich, C. Frontera, A. Roig, M. van Veenendaal, and J. Nogués, "Nonzero orbital moment in high coercivity ε-Fe_2O_3 and low-temperature collapse of the magnetocrystalline anisotropy," Phys. Rev. B **79**, 094404 (2009).
[15]A. Namai, M. Yoshikiyo, K. Yamada, S. Sakurai, T. Goto, T. Yoshida, T. Miyazaki, M. Nakajima, T. Suemoto, H. Tokoro, and S. Ohkoshi, "Hard magnetic ferrite with a gigantic coercivity and high frequency millimetre wave rotation," Nat. Commun. **3**, 1035 (2012).
[16]G. A. Bukhtiyarova, O. N. Martyanov, S. S. Yakushkin, M. A. Shuvaeva, and O. A. Bayukov, "State of iron in nanoparticles prepared by impregnation of silica gel and aluminum oxide with $FeSO_4$ solutions," Phys. Solid State **52**, 826–837 (2010).
[17]G. A. Bukhtiyarova, M. A. Shuvaeva, O. A. Bayukov, S. S. Yakushkin, and O. N. Martyanov, "Facile synthesis of nanosized ε-Fe_2O_3 particles on the silica support," J. Nanopart. Res. **13**, 5527–5534 (2011).
[18]S. S. Yakushkin, A. A. Dubrovskiy, D. A. Balaev, K. A. Shaykhutdinov, G. A. Bukhtiyarova, and O. N. Martyanov, "Magnetic proper ties of few nanometers ε-Fe_2O_3 nanoparticles supported on the silica," J. Appl. Phys. **111**, 044312 (2012).
[19]D. A. Balaev, A. A. Dubrovskiy, K. A. Shaykhutdinov, O. A. Bayukov, S. S. Yakushkin, G. A. Bukhtiyarova, and O. N. Martyanov, "Surface effects and magnetic ordering in few-nanometer-sized ε-Fe_2O_3 particles," J. Appl. Phys. **114**, 163911 (2013).
[20]I. S. Poperechny, Yu. L. Raikher, and V. I. Stepanov, "Dynamic magnetic hysteresis in single-domain particles with uniaxial anisotropy," Phys. Rev. B **82**, 174423 (2010).
[21]I. S. Poperechny and Yu. L. Raikher, "Dynamic hysteresis of a uniaxial superparamagnet: Semi-adiabatic approximation," Physica B **435**, 58–61 (2014).
[22]C. Chen, O. Kitakami, and Y. Shimada, "Particle size effects and surface anisotropy in fe-based granular films," J. Appl. Phys. **84**, 2184–2188 (1998).
[23]V. P. Shilov, J.-C. Bacri, F. Gazeau, F. Gendron, R. Perzynski, and Y. L. Raikher, "Ferromagnetic resonance in ferrite nanoparticles with uniaxial surface anisotropy," J. Appl. Phys. **85**, 6642–6647 (1999).
[24]A. Aharoni, "Surface anisotropy in micromagnetics," J. Appl. Phys. **61**, 3302–3304 (1987).
[25]X. Batlle and A. Labarta, "Finite-size effects in fine particles: Magnetic and transport properties," J. Phys. D: Appl. Phys. **35**, R15–R42 (2002).
[26]M. Jamet, W. Wernsdorfer, C. Thirion, V. Dupuis, P. Mélinon, A. Pérez, and D. Mailly, "Magnetic anisotropy in single clusters," Phys. Rev. B **69**, 024401 (2004).
[27]F. Bødker, S. Mørup, and S. Linderoth, "Surface effect in metallic iron nanoparticles," Phys. Rev. Lett. **72**, 282–285 (1994).
[28]W. F. Brown, "Thermal fluctuations of a single-domain particle," Phys. Rev. **130**, 1677–1686 (1963).
[29]Y. L. Raikher and M. I. Shliomis, "The effective field method in the orientational kinetics of magnetic fluids and liquid crystals," Adv. Chem. Phys. **87**, 595–751 (2007).
[30]N. Pérez, P. Guardia, A. G. Roca, M. P. Morales, C. J. Serna, O. Iglesias, F. Bartolomé, L. M. Garcia, X. Batlle, and F. Labarta, "Surface anisotropy broadening of the energy barrier distribution in magnetic nanoparticles," Nanotechnology **19**, 475704 (2008).